Oral Radiology (2019) 35:11–15
https://doi.org/10.1007/s11282-017-0311-y

ORIGINAL ARTICLE

Prediction of malignancy of submandibular gland tumors with apparent diffusion coefficient

Ahmed Abdel Khalek Abdel Razek[1]

Received: 2 August 2017 / Accepted: 18 December 2017 / Published online: 29 December 2017

Abstract

Objective This study was performed to predict malignancy of submandibular gland tumors using the apparent diffusion coefficient (ADC).

Methods In total, 31 patients (19 male, 12 female; age, 16–71 years) with solid submandibular gland tumors were retrospectively analyzed. All patients underwent single-shot echo-planar diffusion-weighted magnetic resonance imaging of the submandibular gland region. ADC maps of the submandibular gland were reconstructed. The ADC value of the submandibular gland tumors was calculated. A freehand region of interest encompassing the homogenous tumor and solid part of the heterogeneous tumor was established.

Results The mean ADC for submandibular gland malignancy ($1.15 \pm 0.09 \times 10^{-3}$ mm^2/s) was significantly lower than that for benignancy ($1.55 \pm 0.25 \times 10^{-3}$ mm^2/s, $P = 0.001$). An ADC of 1.26×10^{-3} mm^2/s could predict malignancy of submandibular gland tumors with an area under the curve of 0.869, accuracy of 84%, sensitivity of 88%, and specificity of 81%.

Conclusion The ADC is a noninvasive imaging parameter that can be used for prediction of malignancy of submandibular gland tumors.

Keywords Diffusion · Magnetic resonance imaging · Submandibular · Tumor

Introduction

Submandibular gland tumors account for 7–11% of all salivary gland tumors, and approximately 41–54% of tumors at this site become malignant. The most common histopathological subtypes of submandibular gland malignancy are adenoid cystic carcinoma, mucoepidermoid carcinoma, and adenocarcinoma. The most common benign tumor of the submandibular gland is pleomorphic adenoma. Surgery is the method of choice for the treatment of submandibular gland tumors. Accurate prediction of submandibular gland malignancy helps in preoperative mapping of the surgery with an adequate safety margin because the submandibular glands are located adjacent to vital structures. The differentiation of high-risk from low-risk malignancy impacts patients' prognosis and selection of adjuvant radiotherapy for high-risk malignancy [1–6].

Submandibular gland tumors usually present as painless masses, and prediction of malignancy based upon history and clinical findings alone is difficult [2–5]. Some reports have discussed the value of different imaging modalities in the assessment of submandibular gland tumors [3–7]. Ultrasound is the initial imaging modality used for evaluation of submandibular gland tumors, but this is an operator-dependent technique [8–10]. Both routine and advanced magnetic resonance (MR) imaging sequences are used to assess submandibular gland masses, but overlapping of the signal intensity and contrast enhancement exists between malignant and benign salivary gland tumors [11–13]. Although computed tomography can localize submandibular gland tumors, this technique is inaccurate for prediction of malignancy and is associated with radiation exposure [1–4]. Biopsy is an invasive procedure [14]. The apparent diffusion coefficient (ADC) is a quantitative parameter of diffusion-weighted imaging that represents the cellularity of the tumors [15–19]. The ADC is used in characterization of head and neck tumors [15–19], and some reports

✉ Ahmed Abdel Khalek Abdel Razek
arazek@mans.edu.eg

[1] Department of Diagnostic Radiology, Faculty of Medicine, Mansoura University, 203 Elgomheryia Street, Mansoura 13551, Egypt

have discussed its use in evaluation of salivary gland tumors [20–25]. The present study was performed to assess low- versus high-risk salivary gland cancer and diagnose low- and high-risk malignancies using the ADC with the overall aim of predicting malignancy of submandibular gland tumors using the ADC.

Materials and methods

Patients

The institutional review board ethics committee approved this retrospective study, and the need for informed consent was waived. The study involved 34 patients with masses in the submandibular gland. Three patients were excluded because they had cystic lesions. Finally, 31 patients (19 male, 12 female; age range, 16–71 years; mean age, 39 years) with submandibular gland masses were included in the study. The final diagnosis of the submandibular masses was confirmed by histopathological examination after either surgical excision ($n=16$) or fine needle biopsy ($n=15$).

Routine MR imaging

MR imaging was performed with a 1.5-Tesla scanner (Symphony; Siemens Medical Systems, Erlangen, Germany) using a circular-polarized surface head coil. All patients underwent T1-weighted spin-echo images (TR/TE of 800/15 ms) and T2-weighted spin-echo images (TR/TE of 4500/80 ms). The contrast T1-weighted images were obtained after intravenous administration of gadoterate meglumine at 0.5 mL/kg (0.1 mmol/kg) body weight.

Diffusion-weighted MR imaging

Diffusion-weighted MR images were obtained using a multislice spin-echo echo-planar imaging sequence. The imaging parameters were a TR/TE of 10.000/108 ms, field of view of 20×25 cm, acquisition matrix of 256×128, section thickness of 5 mm, and an inter-slice gap of 1–2 mm. Diffusion-weighted MR images were acquired with a diffusion-weighted factor (b) of 0, 500, and 1000s/mm^2. The ADC map was reconstructed by commercially available software. The total time for data acquisition by diffusion-weighted MR imaging was 2 min.

Image analysis

One radiologist (A.A.) with 25 years of expertise in head and neck imaging analyzed the ADC map. A freehand region of interest (ROI) encompassing the homogenous tumor and solid part of the heterogeneous tumor was established. The ROI was smaller than the mass and did not include adjacent normal tissue. The selected ROI exhibited homogeneous intermediate signal intensity on T1- and T2-weighted images and avoided bias from small regions of necrosis/cystic elements, which could give a falsely elevated ADC value (Fig. 1).

Statistical analysis

The data were statistically analyzed using the Statistical Package for the Social Sciences version 20.0 (IBM Corp., Armonk, NY, USA). The statistical significance of the difference between malignancy and benignancy of the

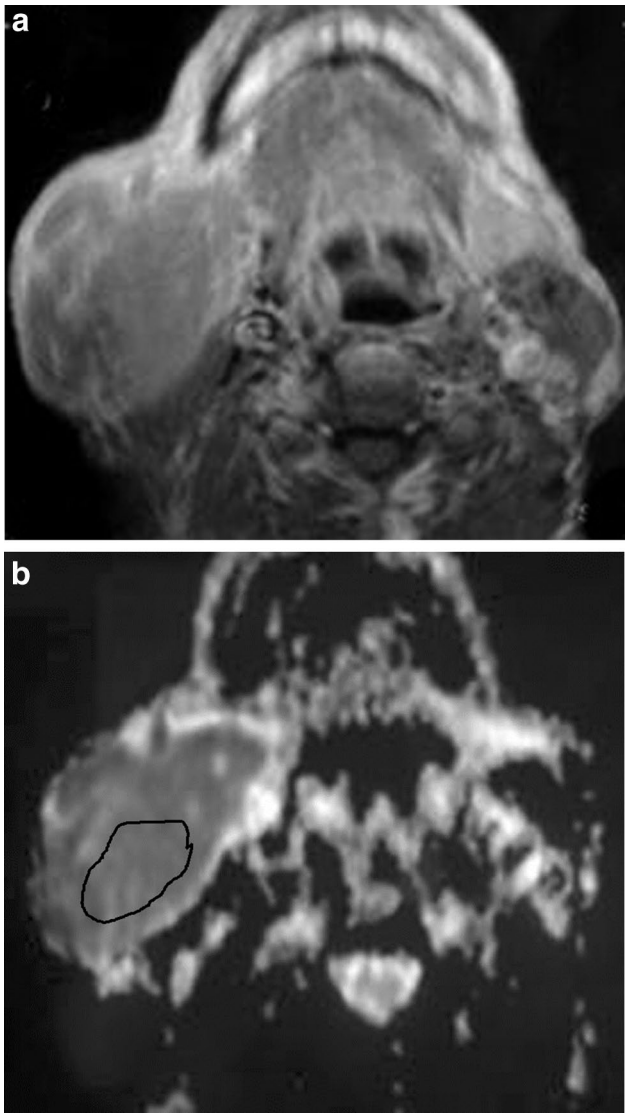

Fig. 1 Mucoepidermoid carcinoma. **a** Axial contrast MR image shows a well-defined mildly inhomogeneously enhanced submandibular mass. **b** ADC map shows region of interest localization with a low ADC for malignancy (1.27×10^{-3} mm^2/s)

submandibular gland tumors was determined. Student's *t* test was used for comparison between two groups. A receiver operating characteristic (ROC) curve was established to determine the cutoff point at which malignancy of submandibular gland tumors could be predicted with highest accuracy.

Results

Table 1 shows the ADC ($\times 10^{-3}$ mm^2/s) of malignancy and benignancy of the submandibular gland tumors.

The mean ADC of submandibular malignancy (Fig. 1) was 1.15 ± 0.09 (0.94–1.27) $\times 10^{-3}$ mm^2/s, and that of benignancy (Fig. 2) was 1.55 ± 0.25 (0.88–1.81) $\times 10^{-3}$ mm^2/s with a significant difference ($P = 0.001$). Selection of an ADC of 1.26×10^{-3} mm^2/s for prediction of malignancy of submandibular tumors resulted in an area under the curve of 0.869, accuracy of 84%, sensitivity of 88%, and specificity of 81% (Fig. 3). There was no significant difference of the ADC within malignant submandibular gland tumors ($P = 0.31$). The lowest ADC (0.94×10^{-3} mm^2/s) of the malignant submandibular tumors was reported in lymphoepithelial carcinoma, and the highest ADC (1.27×10^{-3} mm^2/s) was reported in mucoepidermoid carcinoma.

The high-risk malignant salivary tumors ($n = 9$) were adenoid cystic carcinoma, adenocarcinoma, carcinoma ex pleomorphic adenoma, lymphoepithelial carcinoma, and squamous cell carcinoma. The low-risk malignant salivary tumors ($n = 6$) were mucoepidermoid carcinoma, acinar cell carcinoma, basal cell carcinoma, and salivary duct carcinoma. The mean ADC of the high-risk and low-risk malignancy was 1.12 ± 0.11 (0.94–1.23) and 1.19 ± 0.05 (1.15–1.27) $\times 10^{-3}$ mm^2/s, respectively. The ADC of high-risk malignancy was lower than that of low-risk malignancy, but the difference did not reach statistical significance ($P = 0.13$). The mean ADC of benignancy was $1.55 \pm 0.25 \times 10^{-3}$ mm^2/s with an insignificant difference within histopathological subtypes of benignancy ($P = 0.06$). Two patients with IgG4-related disorders and another patient with a Warthin tumor exhibited restricted diffusion with a low ADC simulating malignancy.

Discussion

The present study has shown that the ADC can predict submandibular gland malignancy with high accuracy. In another study, the ADC map effectively depicted the histologic features of salivary gland tumors, such as the presence of cancer cells, myxomatous tissues, fibrosis, necrosis, cyst formation, and lymphoid tissues [24]. Another study added that the ADC can differentiate pleomorphic adenoma and myoepithelial adenomas from salivary gland malignancy [25]. The low ADC of submandibular gland malignancy is explained by hypercellularity with a decreased extracellular

Table 1 Apparent diffusion coefficient of malignancy and benignancy of submandibular gland tumors

Pathology	Apparent diffusion coefficient
Malignancy ($n = 15$)	1.15 ± 0.09 (0.94–1.27)
High-risk malignancy ($n = 9$)	1.12 ± 0.11 (0.94–1.23)
Adenoid cystic carcinoma ($n = 5$)	1.16 ± 0.09 (0.99–1.23)
Adenocarcinoma ($n = 1$)	1.27
Carcinoma ex pleomorphic adenoma ($n = 1$)	1.14
Lymphoepithelial carcinoma ($n = 1$)	0.94
Squamous cell carcinoma ($n = 1$)	1.15
Low-risk malignancy ($n = 6$)	1.19 ± 0.05 (1.15–1.27)
Mucoepidermoid carcinoma ($n = 3$)	1.20 ± 0.06 (1.16–1.27)
Acinar cell carcinoma ($n = 1$)	1.17
Basal cell carcinoma ($n = 1$)	1.15
Salivary duct carcinoma ($n = 1$)	1.26
Benignancy ($n = 16$)	1.55 ± 0.25 (0.88–1.81)
Pleomorphic adenoma ($n = 5$)	1.74 ± 0.06 (1.65–1.81)
Oncocytoma ($n = 3$)	1.70 ± 0.08 (1.61–1.78)
Schwannoma ($n = 2$)	1.45 ± 0.04 (1.42–1.49)
Basal cell adenoma ($n = 2$)	1.68 ± 0.08 (1.62–1.74)
IgG4-related disorder ($n = 2$)	1.10 ± 0.09 (1.03–1.17)
Myoepithelioma ($n = 1$)	1.52
Warthin tumor ($n = 1$)	0.88

Apparent diffusion coefficient is given in 10^{-3} mm^2/s. Data are presented as mean ± standard deviation (range)

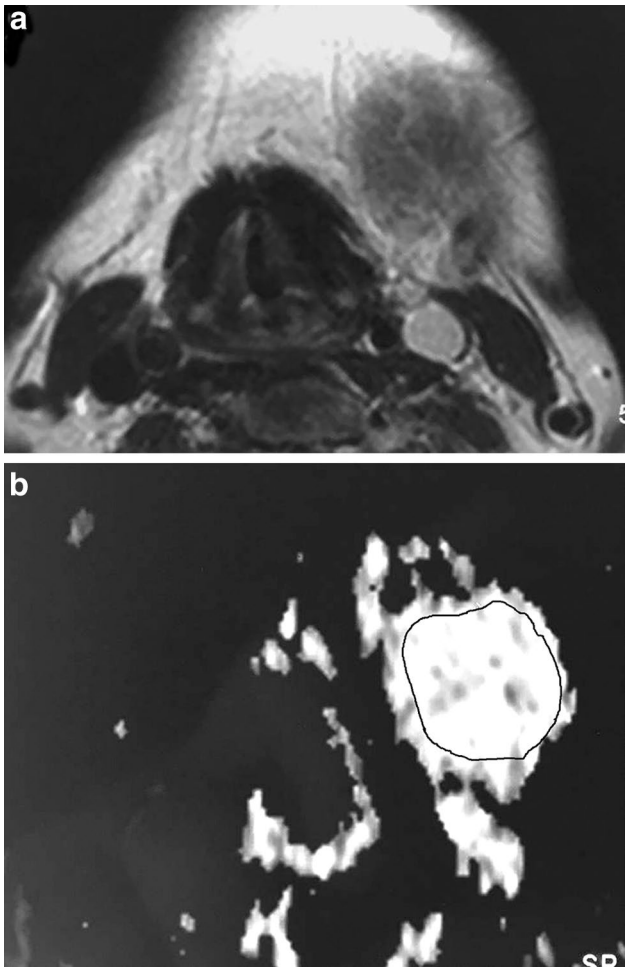

Fig. 2 Pleomorphic adenoma. **a** Axial T2-weighted MR image shows a well-defined mass in the left submandibular region. **b** ADC map shows a high ADC (1.77×10^{-3} mm^2/s)

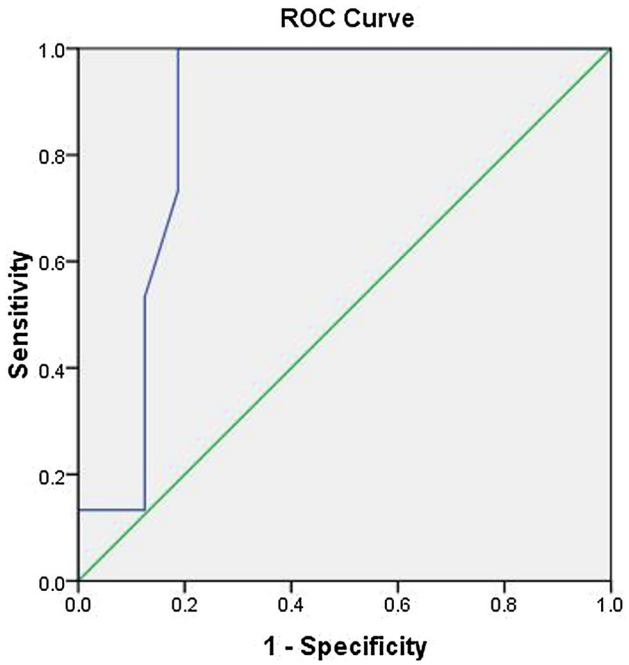

Fig. 3 ROC curve. ADC for prediction of malignancy of submandibular gland tumors is 1.26×10^{-3} mm^2/s with an AUC of 0.869 and sensitivity of 81%

matrix and resultant restricted diffusion. The high ADC of benignancy may be attributed to the lower cellularity with an increased extracellular matrix and resultant unrestricted diffusion [15–21].

In the present study, we found no significant difference in the ADC of subtypes of submandibular gland malignancy, with the highest ADC observed in mucoepidermoid carcinoma and lowest ADC observed in lymphoepithelial carcinoma. Previous studies showed overlap in the ADC of malignant salivary gland tumors without a significant difference in the ADC of histopathological subtypes of malignant tumors [14–17]. One study indicated that the high ADC of mucoepidermoid carcinoma may be attributed to the excess mucous content of the tumor [15]. The low ADC of lymphoepithelial tumors may be related to the presence of highly cellular lymphoid tissue within the tumor with restricted diffusion. Previous studies have shown that lymphomas exhibit restricted diffusion with lower ADCs because of the high cellularity of lymphoid tissue [15].

The biological behavior of submandibular gland malignancy varies according to the histopathological subtype. High-risk malignancy is associated with an aggressive course and high rate of locoregional recurrence. Adjuvant radiotherapy is recommended for patients with high-risk malignancy to improve locoregional control and decrease the incidence of distant metastasis and postoperative recurrence. The 5-year survival rate in patients with high-grade salivary malignancy is 40%, and that in patients with low-grade salivary malignancy is 90% [1–6]. Previous studies have shown an inverse relationship between the ADC and the degree of tumor cellularity [16–18]. In the present study, the ADC of high-risk malignancy was lower than that of low-risk malignancy, but the difference did not reach statistical significance, and a lower ADC could predict high-risk malignancy. The difference in the ADC between low- and high-risk malignancy is attributed to higher cellularity in high- than low-risk malignancy [14–17].

In the present study, the ADC of some benign lesions simulated malignancies. Two patients with IgG4-related disorders showed restricted diffusion and low ADCs of the submandibular gland. This may have been caused by the presence of abundant infiltration of IgG4-positive plasma cells and lymphocytes with excess fibrosis [1–7]. Another patient with a Warthin tumor had restricted diffusion with a low ADC, simulating a malignancy. This may be explained by the presence of a bilayered columnar and basaloid epithelium with a surrounding organized lymphoid stroma containing lymphoid follicles [20–22].

The merits of diffusion-weighted MR imaging of the submandibular gland are that the ADC has an important auxiliary role in MR diagnosis in cases that lack specific findings of malignancy or benignancy and that there is a significant difference in the ADC between low- and high-risk malignancy. The limitations of the ADC are its overlap between benign and malignant submandibular tumors and the lack of standardization of parameters of diffusion-weighted MR imaging.

This study was limited by heterogeneity of different histopathological subtypes of the submandibular gland tumors. Further multicenter studies involving larger numbers of patients with submandibular gland tumors will improve the results. Additionally, this study was conducted using diffusion-weighted MR imaging with a 1.5-Tesla MR scanner. Further studies using multi-parametric MR imaging with dynamic contrast studies and diffusion tensor imaging will improve the results.

We conclude that the ADC is an imaging parameter can be used for prediction of malignancy of submandibular gland tumors.

Compliance with ethical standards

Conflict of interest Ahmed Abdel Khalek Abdel Razek declares no conflict of interest.

Human and animal rights statement This article does not contain any studies with human or animal subjects performed by the author.

References

1. Atula T, Panigrahi J, Tarkkanen J, Mäkitie A, Aro K. Preoperative evaluation and surgical planning of submandibular gland tumors. Head Neck. 2017;39:1071–7.
2. Mizrachi A, Bachar G, Unger Y, Hilly O, Fliss DM, Shpitzer T. Submandibular salivary gland tumors: clinical course and outcome of a 20-year multicenter study. Ear Nose Throat J. 2017;96:E17–E20.
3. Lee RJ, Tan AP, Tong EL, Satyadev N, Christensen RE. Epidemiology, prognostic factors, and treatment of malignant submandibular gland tumors: a population-based cohort analysis. JAMA Otolaryngol Head Neck Surg. 2015;141:905–12.
4. Dalgic A, Karakoc O, Karahatay S, Hidir Y, Gamsizkan M, Birkent H, et al. Submandibular triangle masses. J Craniofac Surg. 2013;24:e529–e31.
5. Ziglinas P, Arnold A, Arnold M, Zbären P. Primary tumors of the submandibular glands: a retrospective study based on 41 cases. Oral Oncol. 2010;46:287–91.
6. Becerril-Ramírez PB, Bravo-Escobar GA, Prado-Calleros HM, Castillo-Ventura BB, Pombo-Nava A. Histology of submandibular gland tumours, 10 years' experience. Acta Otorrinolaringol Esp. 2011;62:432–5.
7. Agarwal AK, Kanekar SG. Submandibular and sublingual spaces: diagnostic imaging and evaluation. Otolaryngol Clin North Am. 2012;45:1311–23.
8. Knopf A, Cortolezis N, Bas M, Mansour N, Hofauer B. Multimodal ultrasonographic algorithm in the differentiation of submandibular masses. Acta Otolaryngol. 2017;137:640–5.
9. Strieth S, Siedek V, Rytvina M, Gürkov R, Berghaus A, Clevert DA. Dynamic contrast-enhanced ultrasound for differential diagnosis of submandibular gland disease. Eur Arch Otorhinolaryngol. 2014;271:163–9.
10. Abdel Razek AA, Ashmalla GA, Gaballa G, Nada N. Pilot study of ultrasound parotid imaging reporting and data system [PIRADS]: inter-observer agreement. Eur J Radiol. 2015;85:2533–8.
11. Kashiwagi N, Murakami T, Nakanishi K, Maenishi O, Okajima K, Takahashi H, et al. Conventional MRI findings for predicting submandibular pleomorphic adenoma. Acta Radiol. 2013;54:511–5.
12. Abdel Razek AA, Samir S, Ashmalla GA. Characterization of parotid tumors with dynamic susceptibility contrast perfusion-weighted magnetic resonance imaging and diffusion-weighted MR imaging. J Comput Assist Tomogr. 2017;41:131–6.
13. Lam PD, Kuribayashi A, Imaizumi A, Sakamoto J, Sumi Y, Yoshino N, et al. Differentiating benign and malignant salivary gland tumours: diagnostic criteria and the accuracy of dynamic contrast-enhanced MRI with high temporal resolution. Br J Radiol. 2015;88:20140685.
14. Taylor MJ, Serpell JW, Thomson P. Preoperative fine needle cytology and imaging facilitates the management of submandibular salivary gland lesions. ANZ J Surg. 2011;81:70–4.
15. Razek AA. Diffusion-weighted magnetic resonance imaging of head and neck. J Comput Assist Tomogr. 2010;34:808–15.
16. Abdel Razek AA, Nada N. Role of diffusion-weighted MRI in differentiation of masticator space malignancy from infection. Dentomaxillofac Radiol. 2013;42:20120183.
17. Abdel Razek A, Mossad A, Ghonim M. Role of diffusion-weighted MR imaging in assessing malignant versus benign skull-base lesions. Radiol Med. 2011;116:125–32.
18. Abdel Razek AA, Kamal E. Nasopharyngeal carcinoma: correlation of apparent diffusion coefficient value with prognostic parameters. Radiol Med. 2013;118:534–9.
19. Razek AA, Sieza S, Maha B. Assessment of nasal and paranasal sinus masses by diffusion-weighted MR imaging. J Neuroradiol. 2009;36:206–11.
20. Terra GT, Oliveira JX, Hernandez A, Lourenço SV, Arita ES, Cortes AR. Diffusion-weighted MRI for differentiation between sialadenitis and pleomorphic adenoma. Dentomaxillofac Radiol. 2017;46:20160257.
21. Assili S, Fathi Kazerooni A, Aghaghazvini L, Saligheh Rad HR, Pirayesh Islamian J. Dynamic contrast magnetic resonance imaging [DCE-MRI] and diffusion weighted MR imaging [DWI] for differentiation between benign and malignant salivary gland tumors. J Biomed Phys Eng. 2015;5:157–68.
22. Tao X, Yang G, Wang P, Wu Y, Zhu W, Shi H, et al. The value of combining conventional, diffusion-weighted and dynamic contrast-enhanced MR imaging for the diagnosis of parotid gland tumours. Dentomaxillofac Radiol. 2017;46:20160434.
23. Attyé A, Troprès I, Rouchy RC, Righini C, Espinoza S, Kastler A, et al. Diffusion MRI: literature review in salivary gland tumors. Oral Dis. 2017;23:572–5.
24. Eida S, Sumi M, Sakihama N, Takahashi H, Nakamura T. Apparent diffusion coefficient mapping of salivary gland tumors: prediction of the benignancy and malignancy. AJNR Am J Neuroradiol. 2007;28:116–21.
25. Habermann CR, Arndt C, Graessner J, Diestel L, Petersen KU, Reitmeier F, et al. Diffusion-weighted echo-planar MR imaging of primary parotid gland tumors: is a prediction of different histologic subtypes possible? AJNR Am J Neuroradiol. 2009;30:591–6.